CHAPTER IV
RESULTS AND DISCUSSION

4.1 CO_2 Absorption by MEA Single Solvent

In this research, the CO_2 absorption from flue gas by using MEA single solvent with various concentrations was firstly investigated to obtain a suitable concentration that provided the high CO_2 removal efficiency and high CO_2 loading capacity.

4.1.1 Effect of Absorption Time

Figure 4.1 shows the change in outlet amounts of CO_2, O_2, and N_2 with respect to absorption time by using the MEA aqueous solutions with various MEA concentrations (20, 25, 30, 35, and 40 wt.%). The absorption system was operated at an initial absorption temperature of 25 °C and a flue gas flow rate of 180 cm^3/min. The O_2 and N_2 concentrations in the outlet gas remained almost invariant, whereas the CO_2 concentration strongly depended on the absorption time. The results clearly indicate that the MEA aqueous solutions selectively absorbed CO_2 rather than O_2 and N_2, even though they could solubilize in the solutions, possibly with low contents under the conditions of continuous flue gas bubbling combined with solution stirring. It can be seen that the absorption time required to reach a maximum CO_2 removal was in the range of 10–30 min. At the MEA concentration of 30 wt.%, the outlet CO_2 amount reached a zero level, which corresponds to 100 % CO_2 removal. It was also found that the high CO_2 removal efficiency at the MEA concentration of 30 wt.% was maintained for a longer absorption time than the other concentrations.

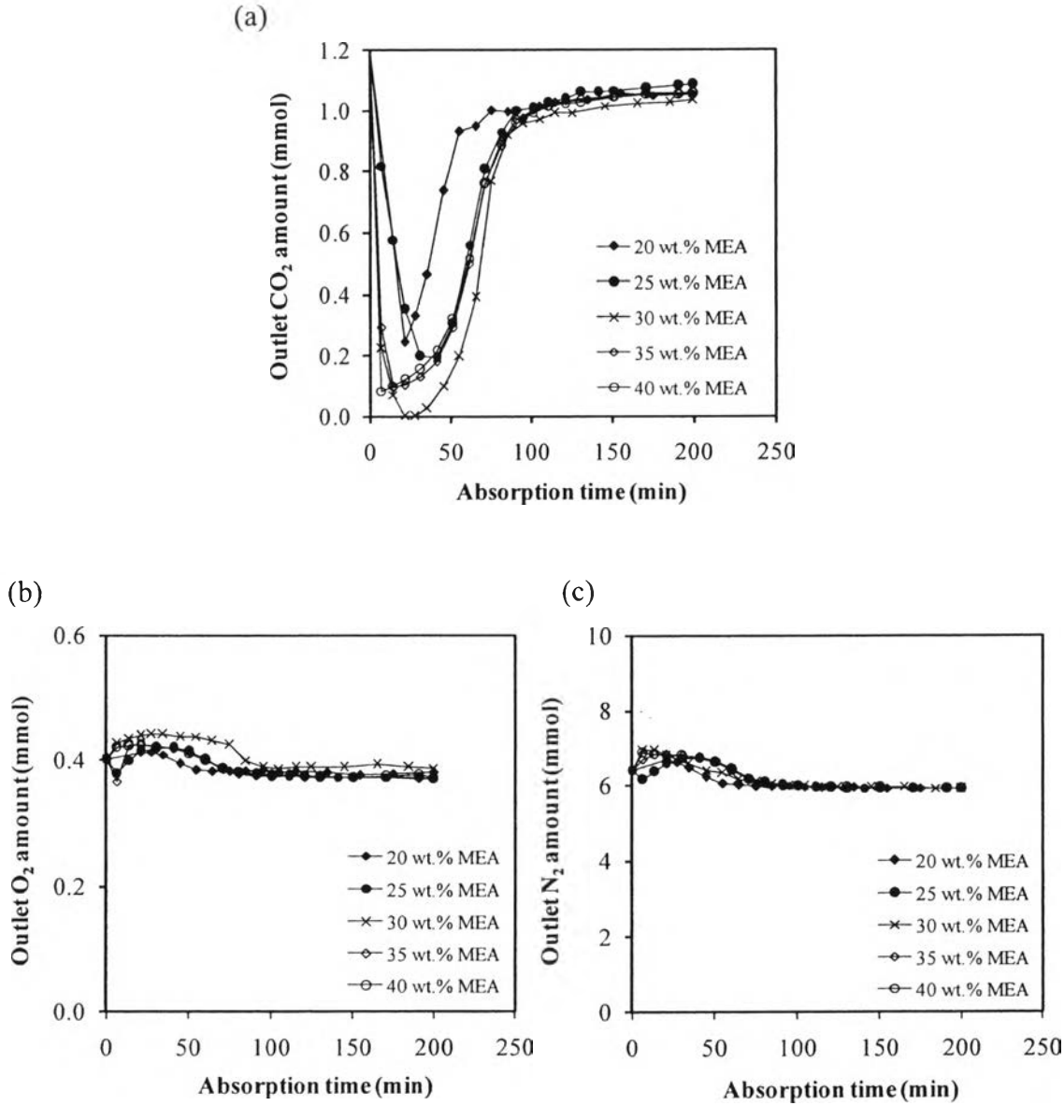

Figure 4.1 Effect of absorption time on outlet amounts of (a) CO_2, (b) O_2, and (c) N_2 using MEA aqueous solutions with various MEA concentrations (Flue gas flow rate of 180 cm^3/min, inlet CO_2 concentration of 15 vol.% (1.2 mmol/min), inlet O_2 concentration of 5 vol.% (0.4 mmol/min), inlet N_2 concentration of 80 vol.% (6.4 mmol/min), MEA concentration of 20–40 wt.%, and initial absorption temperature of 25 °C).

Although the initial absorption temperature was kept constant, the temperature variations in the absorption reactor were unavoidable due to the exothermic reaction between CO_2 and MEA. The temperature variations of MEA solution temperature as a function of absorption time are shown in Figure 4.2. As clearly seen, the temperature variations for all MEA concentrations were in the same trend. The temperature gradually increased to reach a maximum value in the range of 35-40 °C and then decreased to its original controlled temperature of about 25 °C or even slightly lower. The results indicated that the exothermic reaction process was dominant for the CO_2-MEA reaction.

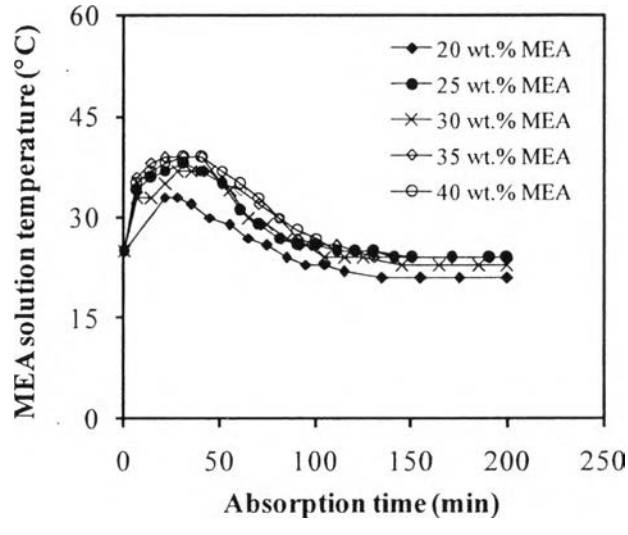

Figure 4.2 Effect of absorption time on temperature of MEA aqueous solutions with various MEA concentrations (Flue gas flow rate of 180 cm^3/min, inlet CO_2 concentration of 15 vol.% (1.2 mmol/min), MEA concentration of 20–40 wt.%, and initial absorption temperature of 25 °C).

The curves shown in Figure 4.1 are quite similar to the breakthrough curves reported in a previous research work (Choi *et al.*, 2009). The point, at which the outlet CO_2 concentration returns to become equal to the inlet CO_2 concentration, is considered to be the breakthrough point for the CO_2 absorption process. When the breakthrough point is reached, the CO_2 absorption can be no longer achieved. The time to reach the breakthrough point for each experiment in this research was

different, depending on the operating conditions. It was experimentally observed that the breakthrough time varied from 100 to 200 min. The total quantity of the absorbed CO_2 was also calculated by using the breakthrough curves, and the CO_2 loading capacity expressed in mol CO_2/mol MEA (or mol CO_2/mol amine in case of blended amines) was then obtained, as explained next.

4.1.2 Effect of MEA Concentration

In order to assess the performance of the MEA aqueous solutions with various MEA concentrations, their maximum CO_2 removal efficiencies are comparatively shown in Figure 4.3. It could be observed that with an increase in MEA concentration from 20 to 30 wt.%, the maximum CO_2 removal efficiency increased from 79.6 to 100 %; however, the maximum CO_2 removal efficiency decreased with further increasing MEA concentration greater than 30 wt.%. Not only the maximum CO_2 removal efficiency but also the CO_2 absorption rate and CO_2 loading capacity would have to be considered for determining the suitable MEA concentration.

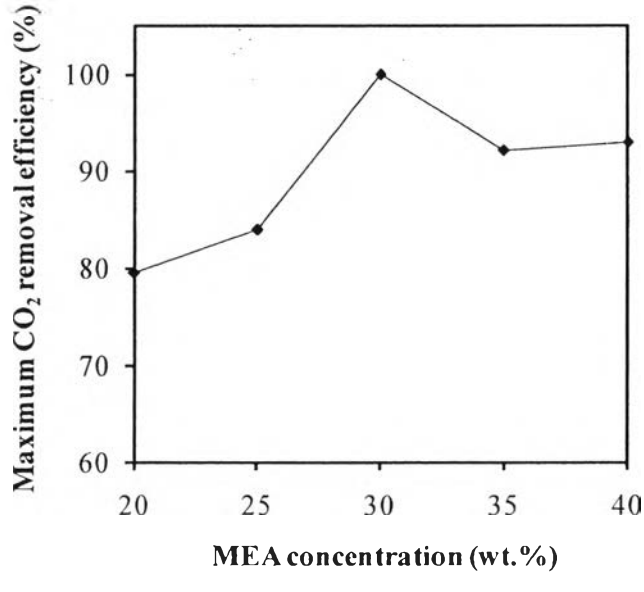

Figure 4.3 Effect of MEA concentration on maximum CO_2 removal efficiency of MEA aqueous solutions (Flue gas flow rate of 180 cm^3/min, inlet CO_2 concentration of 15 vol.% (1.2 mmol/min), MEA concentration of 20–40 wt.%, and initial absorption temperature of 25 °C).

Figure 4.4 shows the CO_2 absorption rate and viscosity of the MEA aqueous solutions with various MEA concentrations. It could be clearly seen that the solution viscosity linearly increased with increasing MEA concentration from 20 to 40 wt.%, whereas the CO_2 absorption rate only slightly decreased with increasing MEA concentration from 20 to 35 wt.% and then sharply decreased with further increasing MEA concentration to 40 wt.%. The results indicate that a limited mass transfer of CO_2 into a more viscous solution at a higher MEA concentration led to a lower CO_2 absorption rate, especially at a very high MEA concentration of 40 wt.%.

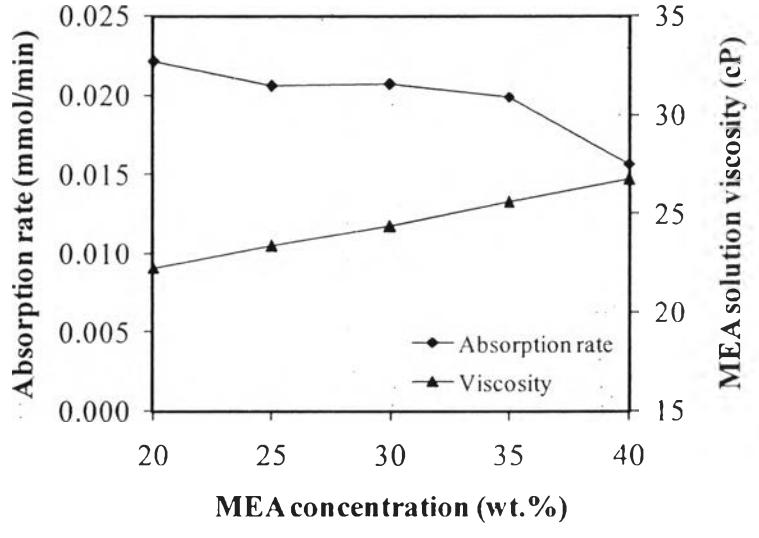

Figure 4.4 Effect of MEA concentration on CO_2 absorption rate and viscosity of MEA aqueous solutions (Flue gas flow rate of 180 cm^3/min, inlet CO_2 concentration of 15 vol.% (1.2 mmol/min), MEA concentration of 20–40 wt.%, and initial absorption temperature of 25 °C).

Moreover, the CO_2 loading capacity of the MEA aqueous solutions with various MEA concentrations is shown in Figure 4.5. It was found that the CO_2 loading capacity was approximately in the range of 0.20–0.35 mol CO_2/mol MEA for the MEA concentration range of 20-40 wt.%. Particularly, when the MEA concentration was greater than 30 wt.%, the CO_2 loading capacity tended to significantly decrease. Theoretically, the CO_2 loading capacity of the MEA aqueous solutions should not be affected by the MEA concentration because the CO_2 loading

capacity of MEA can be as high as the stoichiometry of 0.5 mol CO_2/mol MEA, as expressed in Equations (4.1) and (4.2), in which 2 moles of MEA can be used to extract 1 mole of CO_2.

$$CO_2 + RNH_2 \longleftrightarrow RNH_2^+COO^- \quad \text{(Zwitterions)} \qquad (4.1)$$

$$RNH_2^+COO^- + RNH_2 \longleftrightarrow RNHCOO^- + RNH_3^+ \qquad (4.2)$$

(Carbamate) (Protonated amine)

There are two possible reasons that could make the CO_2 absorption capacity significantly decrease when increasing the MEA concentration higher than 30 wt.%.

1. The reaction rate of MEA for the CO_2 absorption decreases due to the mass transfer limitation since the MEA aqueous solution becomes more viscous at such high MEA concentration.
2. The O_2 molecules in the flue gas lead to a more probability of MEA degradation.

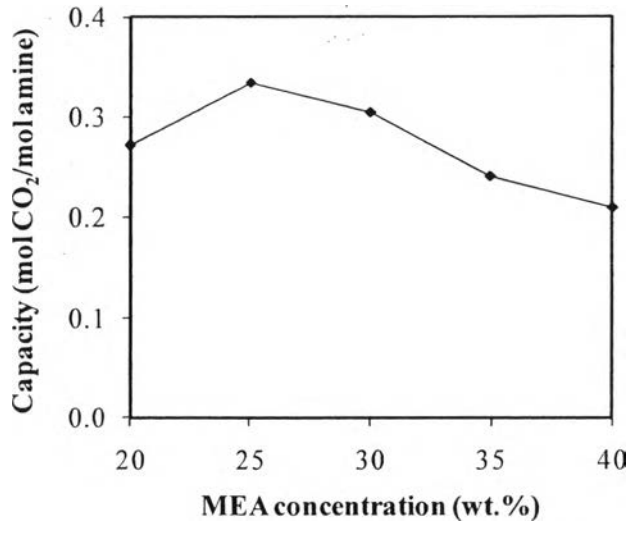

Figure 4.5 Effect of MEA concentration on CO_2 loading capacity of MEA aqueous solutions (Flue gas flow rate of 180 cm^3/min, inlet CO_2 concentration of 15 vol.% (1.2 mmol/min), MEA concentration of 20–40 wt.%, and initial absorption temperature of 25 °C).

In overall, the MEA concentration of 30 wt.% was considered to be the most suitable value for the CO_2 removal from flue gas because of the observed maximum CO_2 removal efficiency, as well as comparatively high CO_2 absorption rate and CO_2 loading capacity.

4.1.3 Effect of Flue Gas Flow Rate

The flue gas flow rate evaluated in this research was in the range of 50-180 cm^3/min due to the precise control limitation of the mass flow controller, whereas the MEA concentration was maintained 30 wt.%. The breakthrough curves of CO_2 absorption at various flue gas flow rates are shown in Figure 4.6. It can be seen that an increase in the flue gas flow rate resulted in a decrease in the breakthrough time. This is possibly because of a faster mass transfer of CO_2 into the solution to react with the MEA. Figure 4.7 shows the effect of flue gas flow rate on the CO_2 absorption rate and CO_2 loading capacity obtained from the breakthrough curves. The results reveal that both the CO_2 absorption rate and CO_2 loading capacity gradually increased with increasing flue gas flow rate. These results imply that the mass transfer limitation was not yet reached under the investigated flue gas flow rate range at the MEA concentration of 30 wt.%, causing a higher CO_2 absorption efficiency at a higher flue gas flow rate. In the other words, the CO_2-MEA reaction possibility more significantly controlled the CO_2 absorption rate and CO_2 loading capacity of the MEA aqueous solution as compared to the mass transfer limitation of CO_2. However, from Figures 4.6 and 4.7, the flue gas flow rate of 50 cm^3/min was selected for further experiments to improve the CO_2 absorption efficiency of the MEA aqueous solution by using other amine additives since its corresponding CO_2 absorption rate and CO_2 loading capacity were not so high that results in any difficulty in the absorption efficiency comparison.

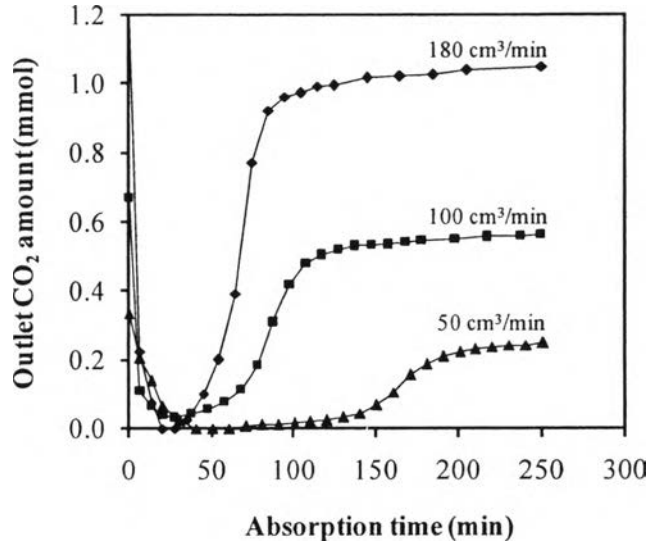

Figure 4.6 Effect of flue gas flow rate on outlet CO_2 amount using MEA aqueous solutions (Inlet CO_2 concentration of 15 vol.%, MEA concentration of 30 wt.%, and initial absorption temperature of 25 °C).

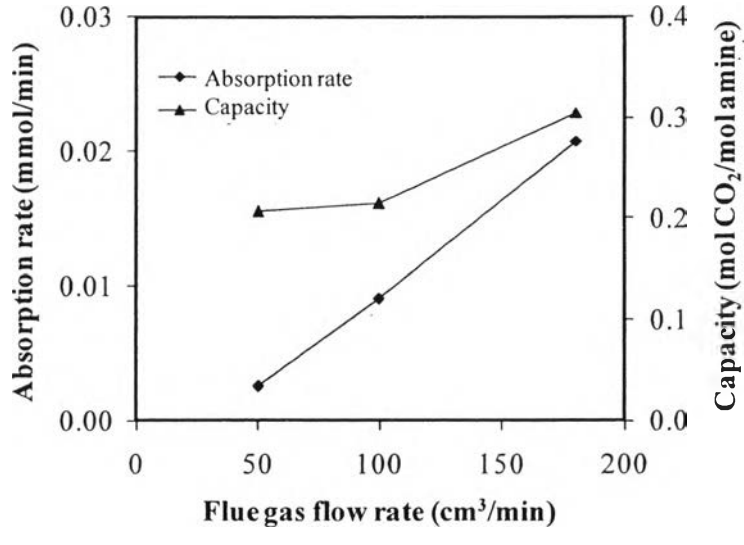

Figure 4.7 Effect of flue gas flow rate on CO_2 absorption rate and CO_2 loading capacity of MEA aqueous solutions (Inlet CO_2 concentration of 15 vol.%, MEA concentration of 30 wt.%, and initial absorption temperature of 25 °C).

4.2 Amine Degradation

Generally, the oxidative degradation of amine requires oxygen or other oxidants and is also catalyzed by iron. This means that the degradation can occur in the presence of dissolved O_2; however, it is not normally encountered in most acid gas-treating systems, such as natural gas purification. Therefore, the degradation process can provide an additional mechanism for MEA degradation specific to CO_2 capture from flue gas as it increases the amine loss and decreases the CO_2 loading capacity. In this research, since the flue gas feed contained 5 vol.% O_2, the experiments were performed to investigate whether or not such O_2 could reduce the CO_2 loading capacity under the operating conditions at atmospheric pressure. To verify the effect of O_2 exposure, the 30 wt.% MEA aqueous solution was saturated with O_2 by thoroughly bubbling overnight with air (containing 21 % O_2 and 79 % N_2) at a flow rate of 40 cm^3/min, at room temperature and atmospheric pressure. Afterwards, the CO_2 absorption rate and CO_2 loading capacity of the 30 wt.% MEA aqueous solutions without and with O_2 exposure were compared.

Figure 4.8 shows the change in outlet amounts of CO_2, O_2, and N_2 with respect to absorption time by using the 30 wt.% MEA aqueous solutions without and with O_2 exposure. It can be clearly seen that the trends of all outlet gases between both cases without and with O_2 exposure were almost exactly the same. Interestingly, the observed distinct difference is that the MEA aqueous solution with O_2 exposure could completely absorb CO_2 at the initial stage (absorption time below 50 min), whereas the only partial CO_2 absorption was detected for the MEA aqueous solution without O_2 exposure. These results can be possibly explained in that the air bubbling may remove some volatile organic contaminants initially presented in the MEA aqueous solution. If that is the case, such volatile organic contaminants may reduce the initial CO_2 absorption efficiency. From the breakthrough curves of CO_2 shown in Figure 4.8(a), the CO_2 absorption rate and CO_2 loading capacity were calculated, and the results are comparatively summarized in Table 4.1. It was surprisingly found that both the CO_2 absorption rate and CO_2 loading capacity of the MEA aqueous solutions without and with O_2 exposure were insignificantly changed. Therefore, it can be concluded that the low O_2 content in the flue gas did not significantly affect

the CO_2 absorption efficiency under the investigated operating conditions at atmospheric pressure.

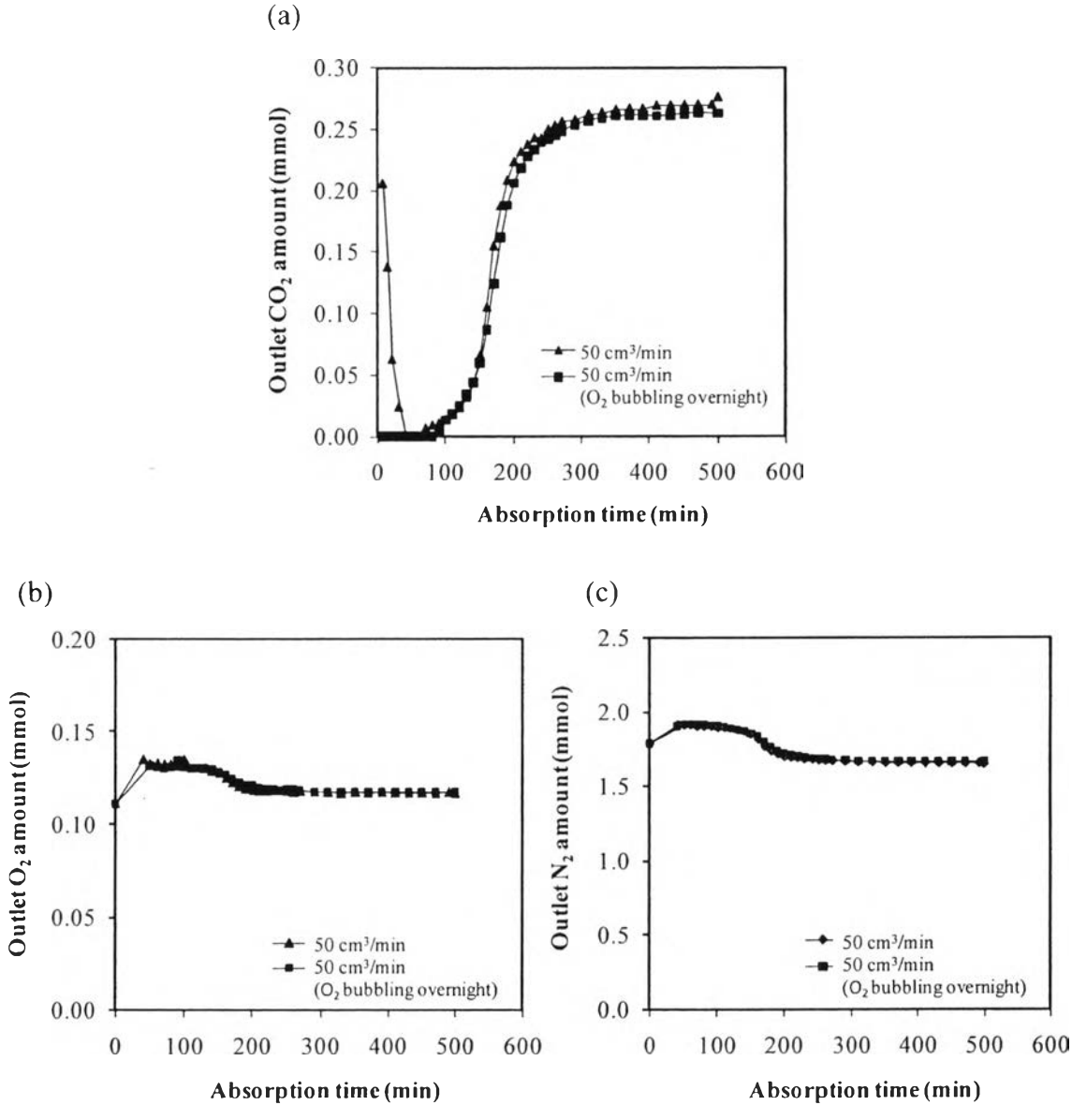

Figure 4.8 Effect of O_2 exposure on outlet amounts of (a) CO_2, (b) O_2, and (c) N_2 using 30 wt.% MEA aqueous solutions (Flue gas flow rate of 50 cm^3/min, inlet CO_2 concentration of 15 vol.% (0.3 mmol/min), inlet O_2 concentration of 5 vol.% (0.1 mmol/min), inlet N_2 concentration of 80 vol.% (1.7 mmol/min), and initial absorption temperature of 25 °C).

Table 4.1 Effect of O_2 exposure on CO_2 absorption rate and CO_2 loading capacity of 30 wt.% MEA aqueous solutions (Flue gas flow rate of 50 cm^3/min, inlet CO_2 concentration of 15 vol.% (0.3 mmol/min), and initial absorption temperature of 25 °C).

Condition	Absorption rate (mmol/min)	CO_2 loading capacity (mol CO_2/mol amine)
Without O_2 exposure	0.0025	0.21
With O_2 exposure	0.0023	0.21

4.3 CO_2 Absorption by Hybrid Solvents

The CO_2 absorption performance of hybrid solvents blended between MEA and sterically hindered amine (AMP, AMPD, and AEPD), as well as diamine (PZ), was next investigated. Such sterically hindered amines and diamine have been proposed as attractive solvents to absorb CO_2 because of their advantages in enhancing the CO_2 loading capacity.

4.3.1 Effect of Blending MEA with Various Amine Additives

Figure 4.9 shows the change in outlet CO_2 amount with respect to absorption time by using the MEA-based aqueous solutions containing 5 wt.% various amine additives in the total amine concentration of 30 wt.%. It can be seen that the absorption time required to reach a maximum CO_2 removal was in the range of 50-120 min, depending on the type of amine additive in the solvent. As compared to the pure MEA aqueous solution, the addition of AMPD, AEPD, and PZ did not affect the maximum CO_2 removal efficiency of 100 % (the point, at which the outlet CO_2 amount reached a zero level), whereas the added AMP slightly decreased the maximum CO_2 removal efficiency to 97.6 %. It can be also interestingly seen that the

MEA-PZ aqueous solution the most improved the CO_2 absorption at the initial stage (absorption time below 50 min).

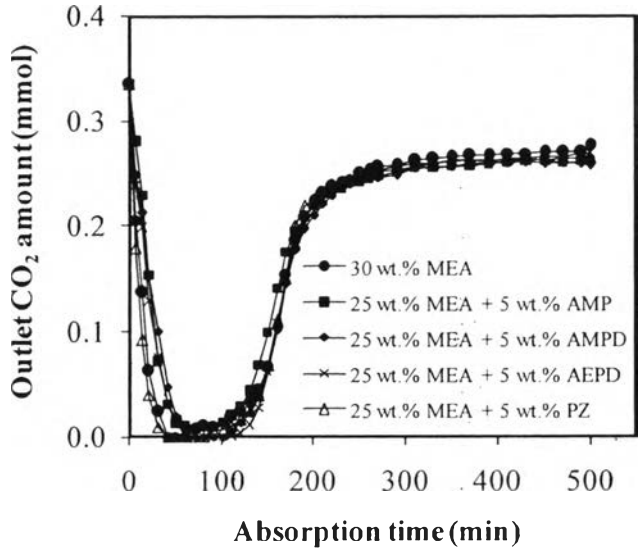

Figure 4.9 Effect of blending MEA with various amine additives on outlet CO_2 amount using MEA-based aqueous solutions containing 5 wt.% various amine additives (Flue gas flow rate of 50 cm^3/min, inlet CO_2 concentration of 15 vol.% (0.3 mmol/min), total amine concentration of 30 wt.%, and initial absorption temperature of 25 °C).

Figure 4.10 shows the effect of type of amine additive on the CO_2 absorption rate and CO_2 loading capacity of the MEA-based aqueous solutions containing 5 wt.% various amine additives. It can be clearly seen that all the investigated amine additives increased both the CO_2 absorption rate and CO_2 loading capacity of the MEA aqueous solution. Particularly, PZ could significantly increase the CO_2 absorption rate because it possessed two amine groups with less structural bulkiness as compared to the other investigated amine additives, as shown in Figure 4.11. However, its limited solubility in an aqueous solution negatively makes it unable to be employed at high concentration, as shown in the next section. Among the investigated sterically hindered amines added to the MEA-based solutions, the CO_2 loading capacity increased in the following order: AMP < AMPD < AEPD.

From Figure 4.11, it can be seen that AMP possesses two methyl substituents at the α-carbon atom as compared to MEA, whereas AMPD possesses one more hydroxyl group than AMP and one less methyl substituent than AEPD at the β-carbon atom. Particularly, the methyl substituent at the α-carbon atom exhibits an electron-withdrawing effect on the amine group (Yoon *et al.*, 2002); therefore, the electron density of nitrogen donor in the amine group is reduced, resulting in the alteration of the CO_2 absorption efficiency. Basically, MEA (a primary amine) dominantly produces carbamate when reacting with CO_2, as shown in Equations (4.1) and (4.2); however, when its hydrogen groups are substituted by other more bulky groups to achieve sterically hindered amines (such as methyl group in the case of AMP), they more preferably produce bicarbonate when reacting with CO_2, as shown in Equation (4.3), due to the instability of the carbamate (Satori and Sawage, 1983). It can be seen that 1 mole of sterically hindered amine can extract 1 mole of CO_2, leading to an increased CO_2 loading capacity as compared to MEA.

$$RNH_2 + CO_2 + H_2O \longleftrightarrow HCO_3^- + RNH_3^+ \qquad (4.3)$$

The carbamate instability of the CO_2-sterically hindered amine reaction implies that the bonding strength between nitrogen atom in the amine group and CO_2 is comparatively weak, possibly resulting from the aforementioned electron withdrawing effect of substituent at the α-carbon atom. When considering the molecular structures of the three investigated sterically hindered amines, the steric hindrance (structural bulkiness) of the substituents bonded to the nitrogen atom in the amine group increases in the following order: AMP < AMPD < AEPD. Therefore, the carbamate stability decreases, while the CO_2 loading capacity increases in such order. The results shown in Figure 4.10 for the three sterically hindered amines as compared to MEA agree very well with this hypothesis. In the case of PZ, despite its less structural bulkiness, the CO_2 loading capacity was not significantly improved as compared to all the investigated sterically hindered amines. However, the CO_2 absorption rate was considerably enhanced, possibly because its two amine groups can more selectively react with CO_2. This can be confirmed by the

temperature of the MEA-PZ aqueous solution, as shown in Figure 4.12, in which its high temperature was maintained for a long absorption period. This indicates a higher probability of MEA-PZ aqueous solution to absorb CO_2 over the studied range of absorption time. Therefore, PZ was selected an effective amine additive to further investigate its suitable content in the MEA-based aqueous solution with the total amine concentration of 30 wt.%.

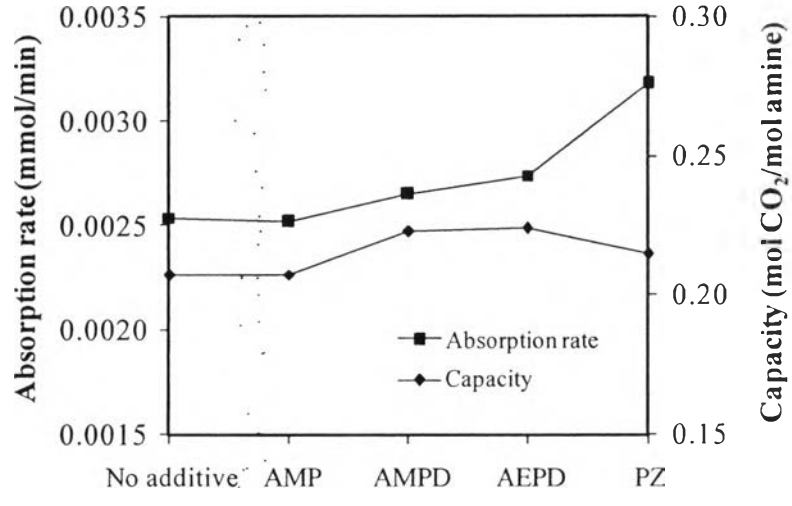

Figure 4.10 Effect of type of amine additive on CO_2 absorption rate and CO_2 loading capacity of MEA-based aqueous solutions containing various 5 wt.% amine additives (Flue gas flow rate of 50 cm^3/min, inlet CO_2 concentration of 15 vol.% (0.3 mmol/min), total amine concentration of 30 wt.%, and initial absorption temperature of 25 °C).

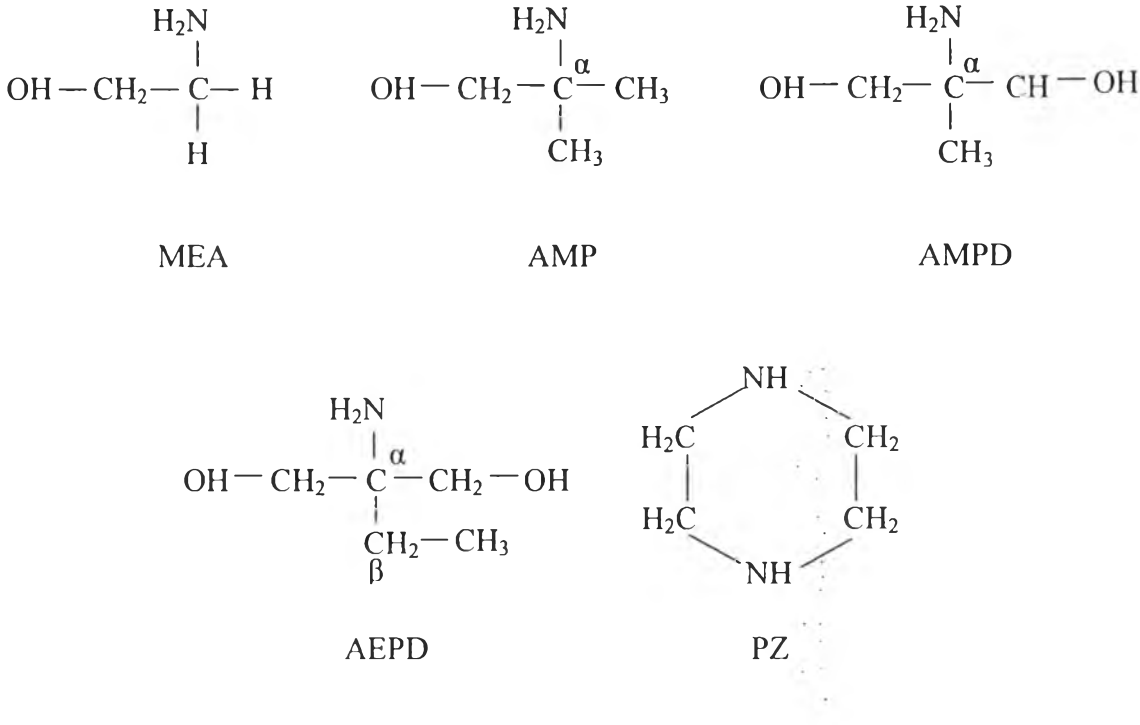

Figure 4.11 Molecular structures of MEA, AMP, AMPD, AEPD, and PZ.

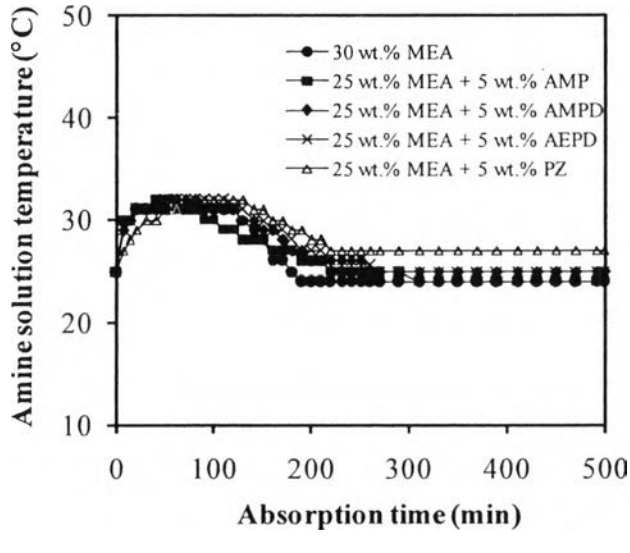

Figure 4.12 Effect of blending MEA with various amine additives on temperature of MEA-based aqueous solutions containing 5 wt.% various amine additives (Flue gas flow rate of 50 cm^3/min, inlet CO_2 concentration of 15 vol.% (0.3 mmol/min), total amine concentration of 30 wt.%, and initial absorption temperature of 25 °C).

4.3.2 Effect of MEA/PZ Ratio

Due to a limited solubility of PZ in the MEA-based aqueous solution as mentioned above, the PZ concentration was varied in the soluble range of 0 to 8 wt.% in the total amine concentration of 30 wt.%, corresponding to various MEA/PZ ratios of 30/0, 27/3, 25/5, and 22/8 wt.%/wt.%. The CO_2 absorption rate and CO_2 loading capacity of the MEA-PZ aqueous solutions containing various MEA/PZ ratios are shown in Figure 4.13. It can be seen that the CO_2 loading capacity tended to gradually increase with increasing the PZ concentration up to 8 wt.%. However, the CO_2 absorption rate increased with increasing PZ concentration to 5 wt.%, whereas the further increase in the PZ concentration up to 8 wt.% reduced the CO_2 absorption rate. These results imply that the high PZ concentration of 8 wt.% enhanced the capacity of CO_2 capture with a comparatively slower rate of reaction. This is possibly because the PZ molecules with two amine groups tend to attract each other and repulse with H_2O molecules at the high PZ concentration (as experimentally observed by the limited solubility of PZ), resulting a slower chance to react with dissolved CO_2 molecules. However, the observed slower absorption rate of PZ at high concentration did not govern its reactivity with CO_2; thus, the CO_2 loading capacity still increased according to the higher number of PZ molecules available. Although the PZ concentration of 5 wt.% provided a lower CO_2 loading capacity than that of 8 wt.%, the former exhibited an acceptably higher CO_2 absorption rate, which is believed to be a prime indicator for the CO_2 removal from the continuously flowing stream of flue gas. Therefore, the MEA/PZ ratio of 25/5 wt.%/wt.% was considered to be an optimum value in this research.

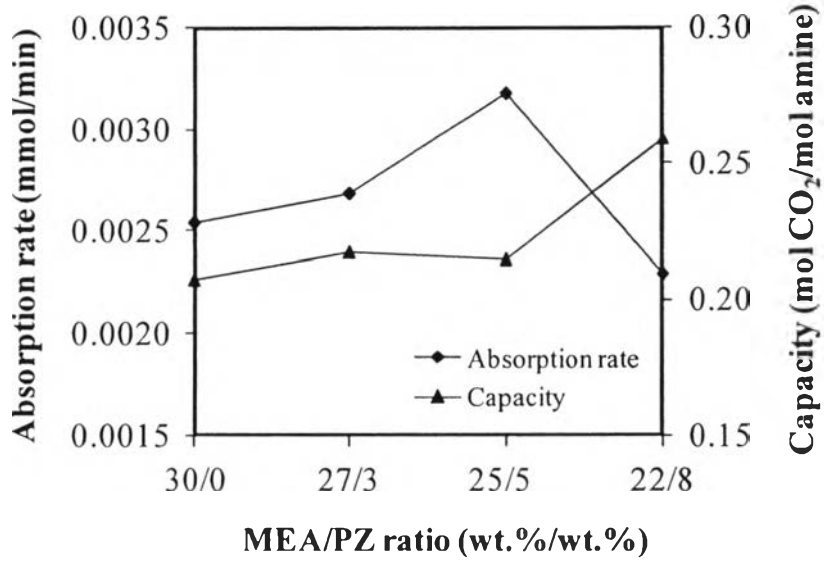

Figure 4.13 Effect of MEA/PZ ratio on CO_2 absorption rate and CO_2 loading capacity of MEA-PZ aqueous solutions (Flue gas flow rate of 50 cm^3/min, inlet CO_2 concentration of 15 vol.% (0.3 mmol/min), total amine concentration of 30 wt.%, and initial absorption temperature of 25 °C).